

EO-polymer waveguide based high dynamic range EM wave sensors

Che-Yun Lin^a, Alan X. Wang^b, Xingyu Zhang^a, Beom Suk Lee^a, and Ray T. Chen^{*a}

^aMicroelectronic Research Center, The University of Texas at Austin, 10100 Burnet Rd, Bldg 160MER, Austin, TX-78758, USA

^bOregon State University, 3097 Kelley Engineering Center Corvallis, OR 97331-5501, USA

ABSTRACT

In this paper, we present the design and experimental demonstration of a high dynamic range electric field sensor based on electro-optic (EO) polymer directional coupler waveguides that offers the strong and ultra-fast EO response of EO polymer. As compared to conventional photonic electric field sensors, our directional coupler waveguide design offers several advantages such as bias-free operation, highly linear measurement response up to 70dB, and a wide electric field detection range from 16.7V/m to 750kV/m at a frequency of 1GHz.

Keywords: photonic sensors, electro-optic polymer, polymer waveguides.

*raychen@uts.cc.utexas.edu; phone 1-(512) 471-7035; Address: 10100 burnet Road, Bldg 160MER, Austin, TX-78758

1. INTRODUCTION

There has been rapidly increasing interest in electric field (E-field) sensors during past decades [1-4]. Electro-magnetic (EM) wave measurement has played a crucial role in various scientific and technical areas, including process control, E-field monitoring in medical apparatuses, ballistic control, electromagnetic compatibility measurements, microwave integrated circuit testing, and detection of directional energy weapon attack. Conventional EM wave measurement systems use active metallic probes, which can disturb the EM waves to be measured and make the sensor very sensitive to electromagnetic noises. Photonic E-field sensors exhibit significant advantages with respect to the electronic ones due to their smaller size, lighter weight, higher sensitivity, and extremely broad bandwidth. Because of these exclusive merits, photonic E-field sensors based on integrated optical devices and optical fibers have emerged in the last ten years [2, 3, 5, 6]. These photonic E-field sensors using Mach-Zehnder (MZ) interferometer or ring resonator, however, offer very limited spurious free dynamic range (SFDR) that are not capable of high fidelity measurement of the EM waves. For example, the inherent nonlinear distortion resulted from the sinusoidal transfer curve make the linearity of a conventional MZ interferometer only to be about 70% [7], which is too small for the EM wave measurement with large dynamic range. Another important limiting factor is that MZ interferometer designs are bias sensitive. The intrinsic sinusoidal optical response to the driving voltage requires the device to be biased at the half power point to achieve the best measurement linearity. The optimum bias point could drift slowly due to charging effects [8], changes in the ambient environment such as the variation of temperature, optical power, and wavelength shifts [9]. This characteristic makes the bias control for MZ interferometer a critical issue, which requires additional bias control circuitry that will inevitably increase the complexity of the device. By contrast, the operation of a Y-fed directional coupler is automatically set at 3dB point, which provides bias free operation. Also, the optical response to the driving voltage can be tailored to achieve very high linearity. These features make Y-fed directional coupler a better candidate for designing a high dynamic range E-field sensor.

2. DESIGN

In this paper, we present the design and experimental results of a photonic E-field sensor based on domain inverted E-O polymer Y-fed directional coupler for electromagnetic wave detection. The Y-fed directional coupler was originally proposed as a linear E-O modulator for RF photonic communication system to achieve a large SFDR [10]. In the following years, more in-depth theoretical investigation was published on how the linearity of a Y-fed directional coupler can be improved by optimizing the lengths and number of the domain inverted sections [11], and experimental results with significantly suppressed intermodulation distortion signals and enhanced SFDR were successfully

demonstrated [12, 13]. We follow the same design principle as our previous work on E-O polymer linear modulator in this paper, but with the removal of the bottom and top electrode to sense the electric field in the free space.

The schematic of the photonic E-field sensor is shown in Figure 1(a). One input waveguide branches into a pair of symmetric waveguides that are optically coupled with each other. Because of the symmetry, equal optical power with the same phase is launched into the coupled waveguides and, hence, the operating point is automatically set at the 3 dB point without any bias voltage. Phase modulation ($\Delta\beta$) reversal can be realized by poling the E-O polymer waveguide with a lumped electrode that zigzags from one waveguide to the neighboring waveguide in the two adjacent domains. This configuration creates an equivalent $\Delta\beta$ reversal without domain-inverted poling of the EO polymer waveguide. The schematic of the cross sectional view shown in Figure 1 (b). After removing the poling electrode, the uniform electric field from free space (far field pattern with wavelength much longer than the E-field sensor dimension) will induce equal phase modulation with reversed polarity. The key design parameters such as the E-O polymer waveguide dimension and the length of the inverted domains exactly follow those in [12, 13].

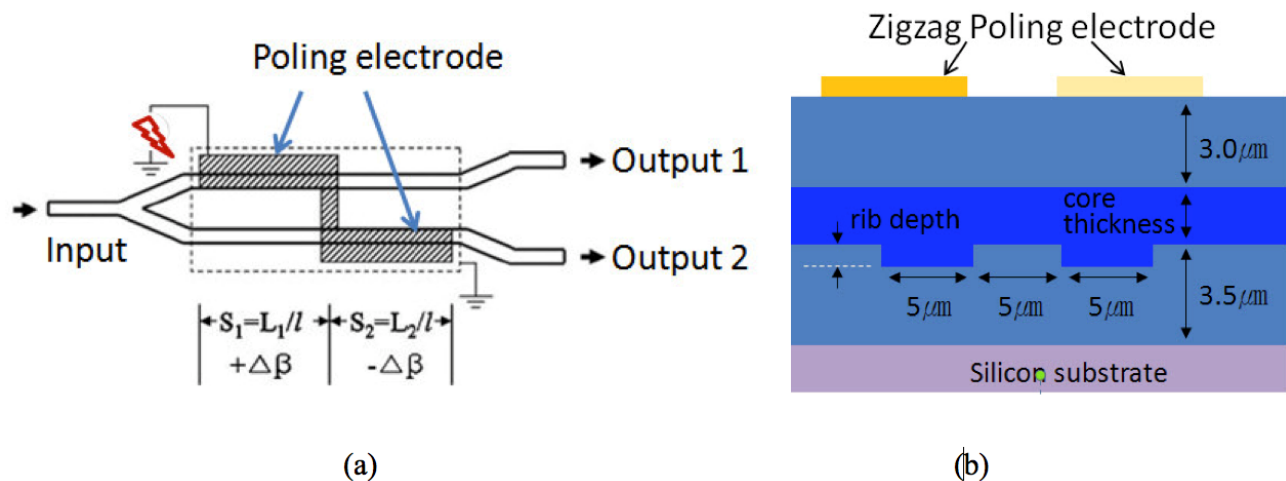


Figure 1. (a) Schematic of the photonic electric field sensor based on domain inverted E-O polymer Y-fed directional coupler (b) Cross sectional view of the directional coupler waveguide with equivalent domain inversion.

3. DEVICE FABRICATION

The photonic E-field sensors are fabricated on silicon wafer carrier. The bottom cladding polymer (UV-15LV) is spin coated and cured to obtain a $3.5\mu\text{m}$ film. Ridge waveguide structures are formed by etching $0.42\mu\text{m} \times 5\mu\text{m}$ trench using reactive ion etching (RIE), and then followed by spin-coating a $1.8\mu\text{m}$ -thick EO polymer layer (excluding the ridge depth). The E-O polymer core layer is made by doping AJ-CKL1 chromophore into amorphous polycarbonate (APC) with 25% weight percentage and then dissolved in cyclopentanone. The solution phase E-O polymer can be spun-on to any substrate and has demonstrated excellent capability to fill narrow trenches [14, 15], which offers great processing simplicity. In the next step, another polymer layer (UFC-170A) is coated on top of the E-O polymer layer and cured to serve as the top cladding. Electrodes for poling are patterned by photolithography, metal deposition, image reversal and lift off. During the poling process, the sample is heated up to the glass transition temperature (T_g) of E-O polymer ($T_g=135^\circ\text{C}$) under a strong DC poling electric field ($100\text{V}/\mu\text{m}$) between the poling electrode and the bottom silicon substrate to align the dipole moment of the E-O polymer molecules. Upon reaching the glass transition temperature, the heater is switched off and the sample is naturally cooled down to room temperature under the same DC electric field. This process freezes the aligned E-O polymer molecules, which preserves electro-optic response of the E-O polymer film without the presence of poling electric field. After poling, the poling electrode is removed by metal etchant. Finally, the photonic E-field sensor devices are diced and polished to for characterization.

4. DEVICE CHARACTERIZATION

The fabricated photonic E-field sensors are tested under a microstrip transmission line that can generate electric field at RF frequency in a direction that is perpendicular to the directional coupler waveguides. The characteristic impedance of

the microstrip line is experimentally measured to be $55.6-j5.4$ without the insertion of the EM wave sensor and $55-j4.9$ with the insertion of the EM wave sensor at 1GHz. The testing setup is shown in Figure 2. The input optical signal coming from a tunable laser source with TM polarization is butt-coupled to the directional waveguide using a polarization maintaining single mode fiber. The output optical signal is collected using a single mode fiber at one branch of the directional waveguide. The measured insertion loss is around 21dB, which corresponds to 6dB propagation loss and 7.5dB/facet coupling loss, respectively. When the RF electrical signal is guided on the microstrip line, it generates electrical field that oscillates in the vertical direction that can modulate the refractive index of the E-O polymer. Similar to an electro-optic modulator for optical communication application, this modulation in refractive index induces the modulation of the output optical signal, which can be detected with a high-speed avalanche photodiode and analyzed with a microwave spectrum analyzer. It is worth noting that the insertion of the EM wave sensor can slightly enhance the electric field by $\sim 9\%$. The uniformity of the electric field under the microstrip line is almost unaffected. Also, due to the difference of the dielectric constant between polymer ($\epsilon_r \sim 3.2$) and air ($\epsilon_r = 1$), the electric field in the polymer layers is $\sim 31\%$ of that in the air.

The disturbance of electric field profile under a microstrip line (MSL) with the insertion of the E-field sensor is also studied. Simulation results in COMSOL Multiphysics show the insertion of the electric field sensor does alter the amplitude of local electric field slightly. Because the thickness of the electric field sensor is small compared to the height of the MSL, the electric field in the air-filled region under the MSL is slightly enhanced by $\sim 9\%$. The uniformity of the electric field under the MSL is almost unaffected as shown in Figure 3. Also, due to the difference of the dielectric constant between polymer ($\epsilon_r \sim 3.2$) and air ($\epsilon_r = 1$), the electric field in the polymer layers would be $\sim 31\%$ of that in the air. This is explained with the simulated potential and electric field distribution shown in Figure 3.

In our experiment, we use 1GHz RF wave as the simulant electric field. The photonic E-field sensors are expected to sense EM waves with much higher frequency in free space (limited by the silicon substrate absorption); however, the microstrip line that we use in our testing setup has significant limited bandwidth due to the skin effect and dielectric absorption. The response from the photonic E-field sensor is shown in Figure 4 with 20dBm RF input power. The photonic E-field sensor shows optical response at the same frequency with 35dB signal to noise ratio (SNR).

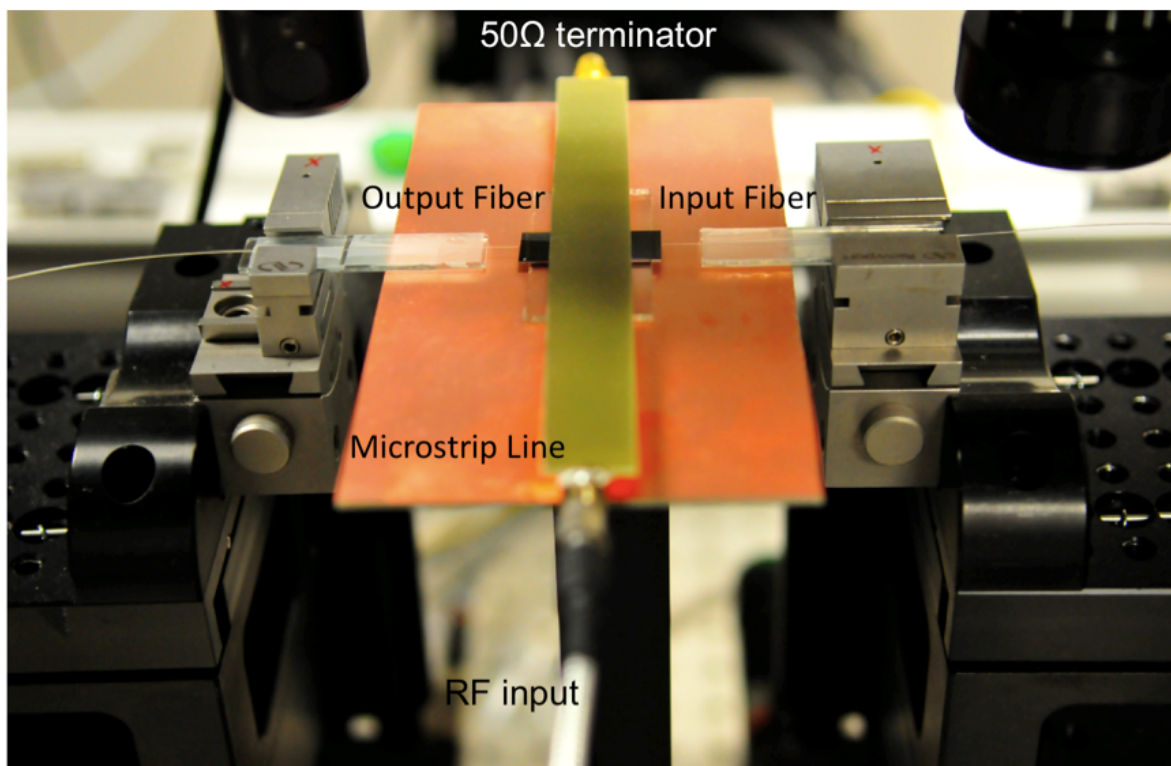


Figure 2. Testing setup for the photonic E-field sensor with the microstrip line that generates vertical electric field, polarization maintaining single mode fiber for input coupling, and single mode fiber for output coupling. The microstrip line

is connected to a RF source with an SMA cable on one end and terminated with a 50ohm terminator on the other end to avoid reflection.

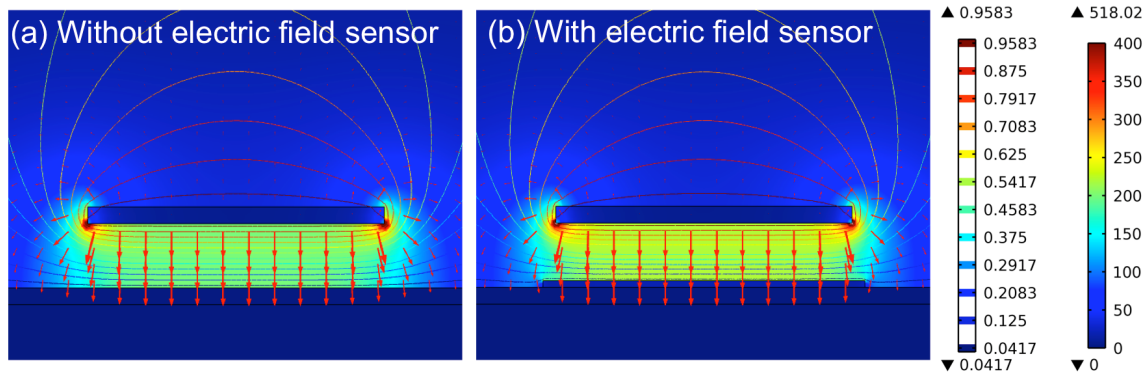


Figure 3. Electric field and potential distribution under the microstrip line used without (a) and with (b) the insertion of or electric field sensor. The contour plot shows the electric potential distribution. The electric field is color-coded and the arrows show its direction.

To test the sensitivity of the photonic E-field sensor, the input RF power is gradually decreased until the sensing signal from the sensor is buried under the noise level. The signal intensity of the photonic E-field sensor is plotted against the input electric field as shown in Figure 5. The electric field E inside the microstrip line can be calculated from the input RF power (P_{in}) [16]: $\vec{E} = \sqrt{2 \cdot P_{in} \cdot Z_0}$, where Z_0 is the characteristic impedance of the microstrip line. The measurement shows that the minimum detectable electric field is found to be 16.7V/m. In our experiment, we measured the electric field up to 550V/m. This is NOT the upper sensing limit of sensor, but simply due to the fact that our RF power source has a maximum output of 20dBm. The variation of the measured curve in Figure 5 is attributed to the instability of optical coupling and laser power fluctuation.

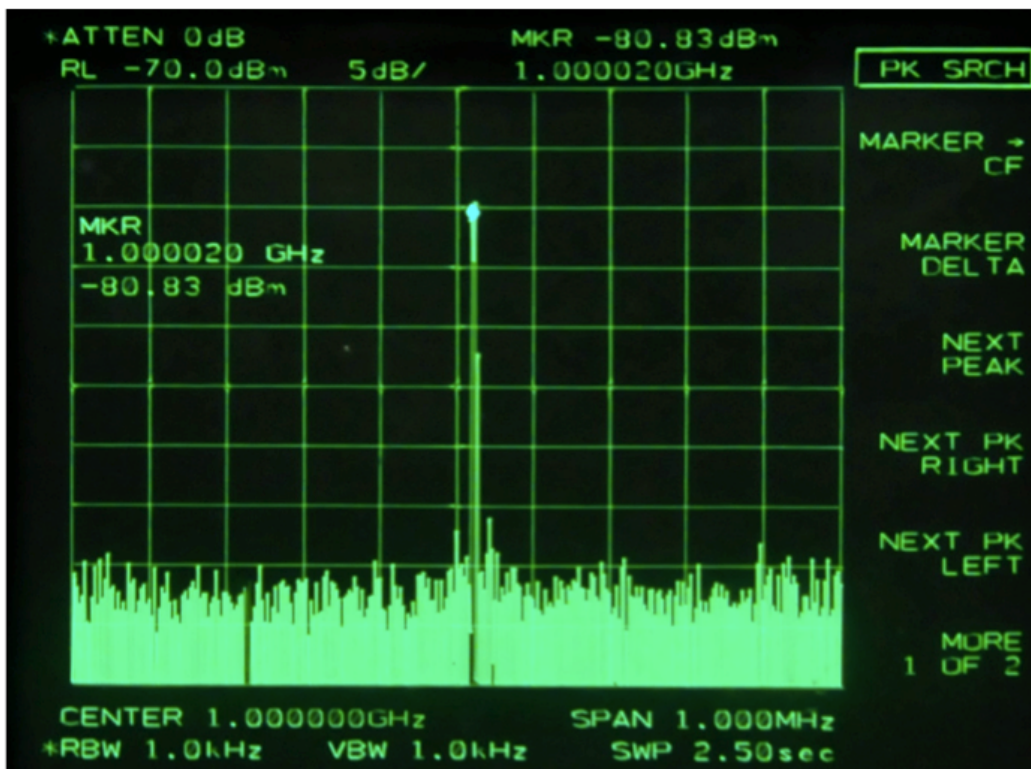


Figure 4. The response of the photonic E-field sensor with 20dBm RF input power at 1GHz.

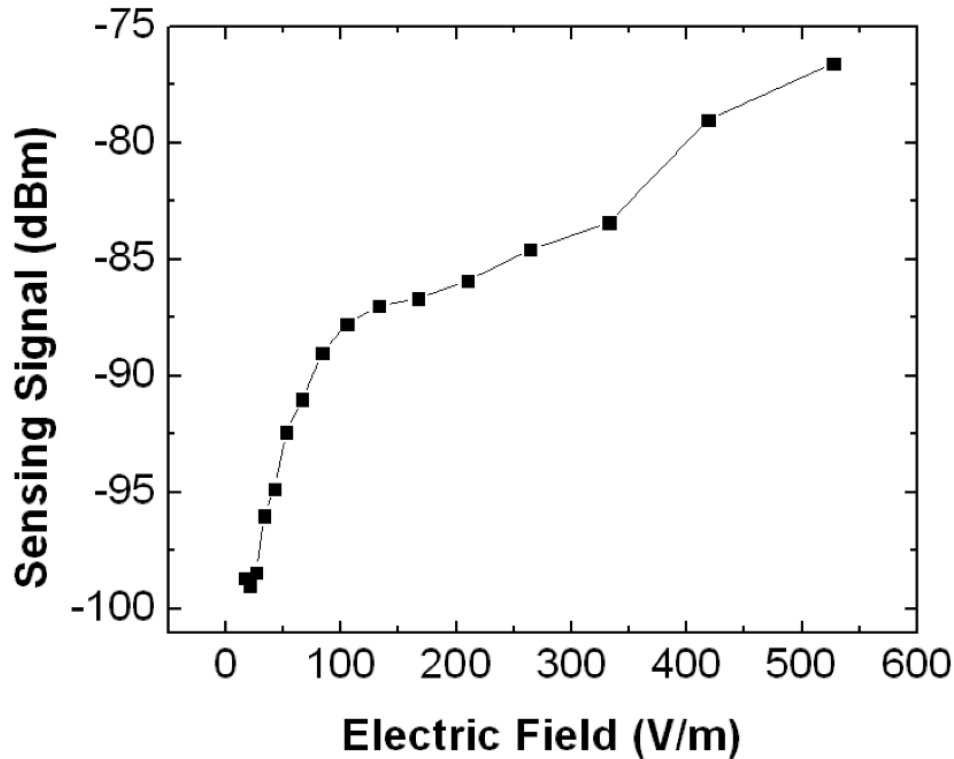


Figure 5. Response from the photonic E-field sensor as a function of the electric field.

In order to determine the maximum electric field the device can sense, we measured another photonic E-field on the same chip without removing the poling electrode on top. By this means, we can apply the driving voltage across a very narrow gap ($\sim 8\mu\text{m}$) to generate a much stronger electric field. The photonic E-field sensor shows over modulation at 6V, which corresponding to an electric field intensity of 750kV/m. Taking consideration of the sensible electric field E from 16.7V/m to 750kV/m, and the Poynting vector of the EM wave is given by $\langle S \rangle = \frac{1}{2} \epsilon_0 \epsilon_r c E^2$, this corresponds to a power range from 1.04W/m^2 to $2.09 \times 10^9\text{W/m}^2$, which is as large as 93dB dynamic range. To measure the spurious free measurement range of the photonic E-field sensor, we use two tone RF signals (100kHz and 105kHz) to drive the sensor with top electrode. It shows the maximum noise free dynamic range of 70dB, which is shown in Figure 6. This result would be of high significance for high fidelity measurement of the EM waves.

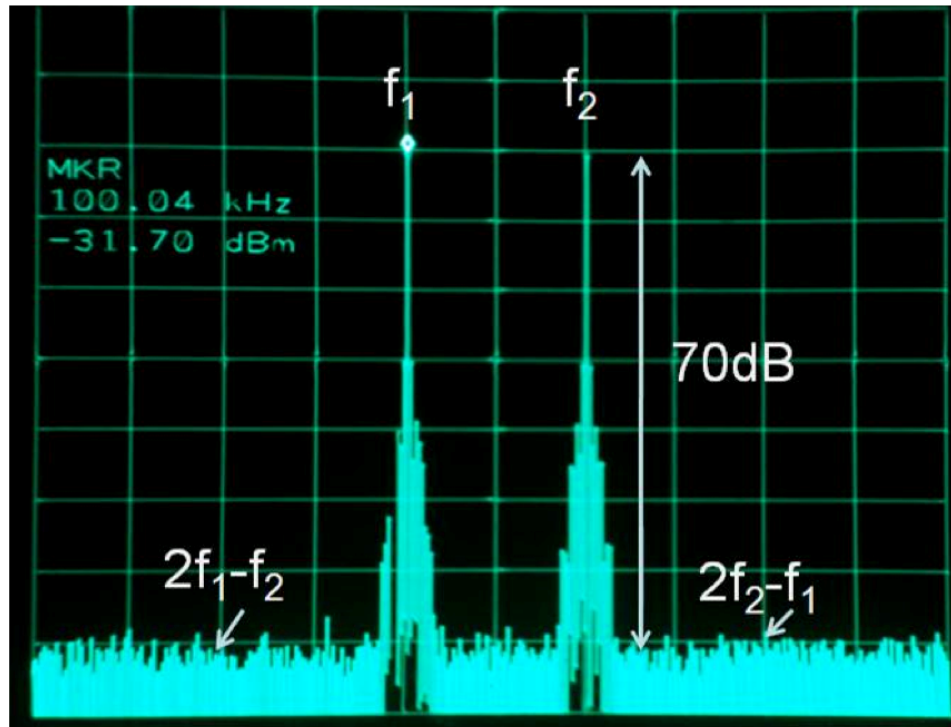


Figure 6. The photonic E-field sensor shows a noise free dynamic range of 70dB.

5. SUMMARY

In conclusion, we have successfully demonstrated electric field sensor based on domain inverted electro-optic (E-O) polymer Y-fed directional coupler for electromagnetic wave detection. The sensor can detect electric field from 16.7V/m to 750kV/m, corresponding to EM waves with large dynamic range of power from 1.04W/m^2 to $2.09 \times 10^9\text{W/m}^2$. The fabricated photonic E-field sensor also achieves a noise free dynamic range of 70dB. Further optimization of E-field sensor through fine tuning the fabrication processes, improving the poling efficiency, and reducing the optical waveguide loss should allow better performance in sensitivity.

6. ACKNOWLEDGEMENT

The authors would like to acknowledge the U.S. ARMY Space & Missile Defense Command/Army Forces Strategic Command (USASMDC/ARSTRAT) for supporting this work under the SBIR grant W9113M-10-P-0076 that is monitored by Dr. Mark Rader.

REFERENCES

- [1] P. Drexler, and P. Fiala, "Methods for High-Power EM Pulse Measurement," IEEE Sensors Journal, 7(7), 1006-1011 (2007).
- [2] N. Kuwabara, K. Tajima, R. Kobayashi *et al.*, "Development and analysis of electric field sensor using LiNbO3 optical modulator," IEEE Transactions on Electromagnetic Compatibility, 34(4), 391-396 (1992).
- [3] S. C. Rashleigh, "Magnetic-field sensing with a single-mode fiber," Optics Letters, 6(1), 19-21 (1981).
- [4] J. Kanwisher, and K. Lawson, "Electromagnetic flow sensors," Limnology and Oceanography, 20(2), 174-182 (1975).
- [5] S. S. Sriram, and S. A. Kingsley, "Sensitivity enhancements to photonic electric field sensor." 5435, 143-152.

- [6] K. Tajima, R. Kobayashi, N. Kuwabara *et al.*, "Optical Fibers and Devices. Development of Optical Isotropic E-Field Sensor Operating More than 10GHz Using Mach-Zehnder Interferometers," *IEICE Trans Electron*, 85(4), 961-968 (2002).
- [7] E. M. Zolotov, and R. Tavlykaev, "Integrated optical Mach-Zehnder modulator with a linearized modulation characteristic," *Quantum Electronics*, 18(3), 401-402 (1988).
- [8] R. L. Jungerman, C. Johnsen, D. J. McQuate *et al.*, "High-speed optical modulator for application in instrumentation," *IEEE Journal of Lightwave Technology*, 8(9), 1363-1370 (1990).
- [9] R. A. Becker, "Circuit effect in LiNbO₃ channel-waveguide modulators," *Optics Letters*, 10(8), 417-419 (1985).
- [10] R. F. Tavlykaev, and R. V. Ramaswamy, "Highly linear Y-fed directional coupler modulator with low intermodulation distortion," *IEEE Journal of Lightwave Technology*, 17(2), 282-291 (1999).
- [11] X. Wang, B.-S. Lee, **C.-Y. Lin** *et al.*, "Electrooptic Polymer Linear Modulators Based on Multiple-Domain Y-Fed Directional Coupler," *Lightwave Technology, Journal of*, 28(11), 1670-1676 (2010).
- [12] B. Lee, C. Y. Lin, A. X. Wang *et al.*, "Linearized electro-optic modulators based on a two-section Y-fed directional coupler," *Applied Optics*, 49(33), 6485-6488 (2010).
- [13] B. Lee, C. Lin, X. Wang *et al.*, "Bias-free electro-optic polymer-based two-section Y-branch waveguide modulator with 22 dB linearity enhancement," *Optics Letters*, 34(21), 3277-3279 (2009).
- [14] X. Wang, C.-Y. Lin, S. Chakravarty *et al.*, "Effective in-device r₃₃ of 735pm/V on electro-optic polymer infiltrated silicon photonic crystal slot waveguides," *Optics Letters*, 36(6), 882-884 (2011).
- [15] C.-Y. Lin, X. Wang, S. Chakravarty *et al.*, "Electro-optic polymer infiltrated silicon photonic crystal slot waveguide modulator with 23 dB slow light enhancement," *Applied Physics Letters*, 97(9), 093304 (2010).
- [16] K. C. Gupta, and I. J. Bahl, "Microstrip lines and slotlines," *Microstrip lines and slotlines*, (1996).